
Single Infection and Dual Co-infection With Respiratory Viruses Affect Cytokine and Chemokine Expression in Acute Respiratory Illness Negative for SARS-CoV-2

[Blanca Guadalupe Gómez-Sotelo](#) , [Evelyn Rivera-Toledo](#) , [Fredy Omar Beltrán-Anaya](#) , [Berenice Illades-Aguilar](#) , [Eugenia Flores-Alfaro](#) , [Daniel Hernández-Sotelo](#) , Adolfo Román-Román , Jorge Gaona-Bernal , [Ramón Antaño-Arias](#) , [Óscar Del Moral-Hernández](#) *

Posted Date: 12 December 2023

doi: 10.20944/preprints202312.0800.v1

Keywords: non-SARS-CoV-2 respiratory viruses; single infection; dual co-infection; viral load; cytokine; chemokine



Preprints.org is a free multidiscipline platform providing preprint service that is dedicated to making early versions of research outputs permanently available and citable. Preprints posted at Preprints.org appear in Web of Science, Crossref, Google Scholar, Scilit, Europe PMC.

Copyright: This is an open access article distributed under the Creative Commons Attribution License which permits unrestricted use, distribution, and reproduction in any medium, provided the original work is properly cited.

Article

Single Infection and Dual Co-Infection with Respiratory Viruses Affect Cytokine and Chemokine Expression in Acute Respiratory Illness Negative for SARS-CoV-2

Blanca Guadalupe Gómez-Sotelo ¹, Evelyn Rivera-Toledo ², Fredy Omar Beltrán-Anaya ^{1,6}, Berenice Illades-Aguiar ^{3,6}, Eugenia Flores-Alfaro ⁴, Daniel Hernández-Sotelo ⁵, Adolfo Román-Román ⁶, Jorge Gaona-Bernal ⁷, Ramón Antaño-Arias ³ and Óscar Del Moral-Hernández ^{1,6,*}

¹ Laboratorio de Virología, Facultad de Ciencias Químico Biológicas, Universidad Autónoma de Guerrero, Chilpancingo 39070, Mexico; blancagomez@uagro.mx (B.G.G.-S.); frebeltran@hotmail.com (F.O.B.-A.)

² Laboratorio de Inmunomodulación y agentes patógenos, Departamento de Microbiología y Parasitología, Facultad de Medicina, Universidad Nacional Autónoma de México, Mexico City 04510, Mexico; evelyn.rivera@unam.mx (E.R.-T.)

³ Laboratorio de Biomedicina Molecular, Facultad de Ciencias Químico Biológicas, Universidad Autónoma de Guerrero, Chilpancingo 39070, Mexico; billades@uagro.mx (B.I.-A.); ramon.a@uagro.mx (R.A.-A.)

⁴ Laboratorio de Epidemiología Clínica y Molecular, Facultad de Ciencias Químico Biológicas, Universidad Autónoma de Guerrero, Chilpancingo, 39070, Mexico; eugeniaflores@uagro.mx (E.F.-A.)

⁵ Laboratorio de Epigenética del Cáncer, Facultad de Ciencias Químico Biológicas, Universidad Autónoma de Guerrero, Chilpancingo 39070, Mexico; dhernandez@uagro.mx (D.H.-S.)

⁶ Laboratorio de Diagnóstico e Investigación en Salud, Facultad de Ciencias Químico Biológicas, Universidad Autónoma de Guerrero, Chilpancingo, 39070, Mexico; arroman6046@gmail.com (A.R.-R.)

⁷ Centro Universitario de Ciencias de la Salud, Departamento de Microbiología y Patología, Universidad de Guadalajara, Guadalajara, Jalisco 44340, Mexico; jorge.gaona@academicos.udg.mx (J.G.-B.)

* Correspondence: odelmoral@uagro.mx

Abstract: During the COVID-19 pandemic, the circulation of non-SARS-CoV-2 respiratory viruses changed throughout the world. This study aimed to analyze the effect of respiratory syncytial virus (RSV), metapneumovirus (MPV), rhinovirus (RV), and parainfluenza (PIV)-3 single infection, dual co-infection, and viral load on cytokine and chemokine expression in 300 Mexican patients with ARIs negative for SARS-CoV-2. Molecular detection and viral load were performed by RT-qPCR. Cytokine and chemokine expression was determined in samples positive for single RSV, MPV, RV, or PIV-3 infection, and in the most frequent dual co-infections, by a cytokine panel using a magnetic-bead-based multiplex immunoassay. Of the patients positive for viral infection, 91.7% had a single infection and 8.3% had dual co-infections. In this study, RSV was the respiratory virus with the highest prevalence, and the most common dual co-infection was RV+RSV. On the other hand, RV infections had the highest viral loads compared to the other viruses detected. FGF basic, MIP-1 α IL-8, IP-10, MCP-1, IFN- γ , and RANTES showed differential expression between single infections and dual co-infections compared to healthy patients. We report, for the first time, the circulation of non-SARS-CoV-2 viruses in the south of Mexico and the cytokine and chemokine profiles associated with these viruses.

Keywords: non-SARS-CoV-2 respiratory viruses; single infection; dual co-infection; viral load; cytokine; chemokine

1. Introduction

Acute respiratory illnesses (ARIs) are an important cause of mortality in children under 5 years old worldwide [1]. The main etiologies are RNA viruses such as human coronaviruses, influenza

viruses, metapneumovirus (MPV), parainfluenza virus (PIV), rhinovirus (RV), and respiratory syncytial virus (RSV) [2]. Most of these respiratory viruses exhibit a pattern of seasonal circulation, and their outbreaks occur in spring and autumn, with peak incidences in the winter months in temperate regions and during the rainy season in tropical regions [3–5].

Non-pharmaceutical interventions (NPIs) used during the COVID-19 pandemic caused by the SARS-CoV-2 virus reduced the circulation of non-SARS-CoV-2 respiratory viruses, including RSV [6]. RSV is a member of the family *Paramyxoviridae* and genus *Pneumovirus* containing a single-stranded non-segmented, negative-sense RNA genome [7,8]. Before the COVID-19 pandemic, RSV was the most common cause of lower respiratory tract infection in the pediatric population and an important cause of hospitalization in adults and the elderly in Latin America [9,10]. In Mexico, RSV is the leading cause of severe ARIs in preterm infants and adults [11,12], it has been detected in co-infection with SARS-CoV-2 [13] and circulating with other RNA respiratory viruses, such as RV, MPV, and PIV [14,15].

RV is a non-enveloped positive-strand RNA virus in the family *Picornaviridae*, genus *Enterovirus* [16]. RV causes more than 50% of upper respiratory tract infections in humans worldwide and is the main etiologic agent of the common cold [17]. RV infections can cause wheezing in all age groups and exacerbations of asthma in both children and adults [18]. Furthermore, RV was the main co-circulating respiratory virus during the COVID-19 pandemic [19,20]. On the other hand, MPV is an enveloped negative-stranded RNA virus with a non-segmented genome belonging to the order *Mononegavirales*, family *Pneumoviridae*, and genus *Metapneumovirus* [21,22]. MPV is an important etiological agent of ARIs in children, adults, and elderly and immunocompromised patients [23]. Before the COVID-19 pandemic, a study reported that MPV circulated mainly in infants under 12 months and adults between the ages of 26 and 59 years [24]. In contrast, during the COVID-19 outbreak, a higher infection rate of MPV in young children than in older adults was observed [25]. Finally, PIV is an enveloped, negative-sense, single-stranded RNA virus that belongs to the family *Paramyxoviridae*. It is classified into four serotypes (PIV-1, PIV-2, PIV-3, and PIV-4) and subdivided into two genera, *Respirovirus* (PIV-1 and PIV-3) and *Rubulavirus* (PIV-2 and PIV-4) [26,27]. PIV is an important cause of upper (URTIs) and lower respiratory tract infections (LRTIs) in infants, young children, the elderly, the immunocompromised, and hematopoietic stem cell transplant patients. It is classified into four serotypes (PIV-1, PIV-2, PIV-3, and PIV-4) [26], and of the four serotypes, PIV-3 is the most virulent, causes 60-70% of PIV infections [28], and has been detected in co-infection with SARS-CoV-2 in children and adults [29,30].

The innate immune response plays an important role in defense against respiratory viruses. The innate immune response signaling cascade begins with the recognition of pathogen-associated molecular patterns by pattern recognition receptors (PRRs). For RNA viruses, the toll-like receptors (TLRs) 3, 7, and 8 and, cytosolic RNA sensors, such as melanoma differentiation-associated gene 5 (MDA5) and retinoic acid-inducible gene I (RIG-I), are the most important pattern recognition receptors (PRRs) [31]. These receptors are expressed in the respiratory epithelial cells and tissue-resident immune cells. Upon viral sensing, the PRRs activate signaling pathways that trigger the release of type I and III IFNs, pro-inflammatory cytokines (TNF- α , tumor necrosis factor-alpha; IL-6, interleukin-6; IL-1 β , interleukin-1 beta; G-CSF, granulocyte colony-stimulating factor, and GM-CSF, granulocyte-macrophage colony-stimulating factor), and chemokines (MCP-1, monocyte chemoattractant protein-1; CXCL9, C-X-C motif chemokine ligand 9 and, IP-10, IFN- γ inducible protein-10) that assist in the prevention and clearance of respiratory viral infections [32]. On the other hand, viral load is one of the important determinants of disease transmission. Additionally, high viral loads of some respiratory viruses are correlated with the severity of illness [33]. For example, a higher SARS-CoV-2 viral load is significantly associated with disease severity and increased risk of mortality [34,35]. For RSV, although some studies have demonstrated that the viral load has a positive correlation with clinical symptoms in children <5 years of age [36], there is no correlation between a high viral load and increased severity of the disease [37]. Herein, we analyze the effect of non-SARS-CoV-2 respiratory viruses, such as single RSV, MPV, RV, and PIV-3 infection, dual co-infection, and

viral load on cytokine and chemokine expression in a population with ARIs negative for SARS-CoV-2 in the south of Mexico during the COVID-19 pandemic.

2. Materials and Methods

2.1. Design and Study Population

This study was conducted from April 17, 2020, to May 24, 2021, in the Virology Laboratory and the Diagnostic and Health Research Laboratory of the Universidad Autónoma de Guerrero, in the State of Guerrero, located in the South of Mexico. This study included pediatric and adult patients with acute respiratory illness, and an operational definition of a suspected case of COVID-19, according to the operational definitions of COVID-19 cases, of Instituto Mexicano del Seguro Social, in Mexico [38]. The nasopharyngeal swab was taken from each individual from which RNA extraction and RT-qPCR were performed for SARS-CoV-2, according to the Berlin Protocol modified by the Instituto de Diagnóstico y Referencia Epidemiológicos Dr. Manuel Martínez Báez (InDRE) of Mexico for the amplification of E and RdRP genes [39]. A total of 5,996 patients with acute respiratory illness were enrolled. A total of 60.1% (3, 449) were negative for the molecular diagnosis of SARS-CoV-2, and of these, 300 patients were selected. The clinical characteristics of the 300 patients selected were obtained from medical records (Supplementary Table 1). A total of 52.5% (157) of the patients were women, 53.9% (160) were in the age group of 24-44 years, and more than 90% were patients without co-morbidities (Supplementary Table 2).

2.2. RT-qPCR and viral load for non-SARS-CoV-2 respiratory viruses

Samples negative for SARS-CoV-2 were processed for molecular detection by RT-qPCR for Influenza A H1N1, differential diagnosis, and viral load of RSV, MPV, RV, and PIV-3 using predesigned hydrolysis probes [39,40]. The SuperScript III Platinum One-Step qRT-PCR Kit (Invitrogen, Cat. 11732088) was used in a CFX96 Touch Real-Time PCR Detection System (Bio-Rad, Cat. 1855195) for amplification of the viral genes. RNAsa P gene amplification was considered an internal control. The primers and probes used for each virus are reported in Supplementary Table 3. The cycle threshold (Ct) values >37 were considered negative. For viral load quantification, a standard curve was plotted using serial dilutions of a concentration standard of RSV (ATCC, VR-26), MPV (ATCC, VR3250SD), RV (ATCC, VR1559DQ), and PIV-3 (ATCC, VR93D). Linear regression analysis was performed to calculate the PCR efficiency and correlation coefficient based on the standard curve of each virus. Ct values of the samples were interpolated within the standard curve, and the logarithms of the initial concentrations were calculated ($\text{Log SQ} = (\text{Ct} - b) / m$), wherein Ct is the threshold cycle, b is the intersection, and m is the slope of the standard curve. The viral load was expressed as log₁₀ RNA copies per microliter (μL).

2.3. Multiplex immunoassay of cytokines and chemokines

Cytokine and chemokine expression was determined in samples positive for RSV, MPV, RV, or PIV-3 infection and in the most frequent viral dual co-infections, by a cytokine panel using a magnetic-bead-based multiplex immunoassay (Bio-Plex Pro Human Cytokine 27- Plex Assay, Bio-Rad, Cat. M500KCAF0Y) according to the manufacturer's instructions. For this analysis, 17 samples single-positive for VSR (29.4%,5/17), MPV (29.4%,5/17), RV (23.5%,4/17), and PIV-3 (17.6%,3/17) were included, in addition to 9 positive samples for the most frequent dual co-infections. SARS-CoV-2-positive samples were also analyzed, including five single-positive and two co-infections between SARS-CoV-2 and PIV-3 (unique dual co-infection detected in nasopharyngeal swabs from our COVID-19 biobank). Nasopharyngeal swabs from three healthy individuals were incorporated as negative controls. Cytokine concentrations (pg/mL) were determined in duplicate analysis for each sample, using an automated immunoassay analyzer.

2.4. Data analysis

The data were analyzed using STATA version 16.1 software (StataCorp LLC, College Station, TX). Cytokine and chemokine expression was analyzed by one-way ANOVA applied to normally distributed data, while the Kruskal–Wallis test was applied to the rest. Comparative analysis was performed using Dunnett's or Dunn's multiple comparison tests, and the correlation between differentially expressed cytokines and chemokines and the viral load was determined using the Spearman correlation coefficient. A p -value of ≤ 0.05 was considered significant.

3. Results

3.1. RSV was the most frequent non-SARS-CoV-2 respiratory virus in the population with ARIs, and RV was the most common virus in dual co-infections

In order to determine the frequency of non-SAR-CoV-2 respiratory viruses in the south of Mexico during the COVID-19 pandemic, molecular detection by RT-qPCR was performed for Influenza A H1N1, RSV, MPV, RV, and PIV-3 in 300 nasopharyngeal swabs from patients with ARIs, negative for SARS-CoV-2. Single infections and dual co-infections were determined. Thirty-six percent (108/300) of the ARIs were positive for RSV, MPV, RV, and PIV-3, whereas no positive cases for influenza A H1N1 were detected. Single infections were identified in 91.7% (99/108) of the samples, and co-infections by two viruses were present in 8.3% (9/108). RSV (20.7%, 62/300) was the most frequent respiratory virus, followed by MPV (9.3%, 28/300) and RV (4%, 12/300) (Figure 1A). RV was recurrent in the co-infections, and the most common of them was RV+RSV (45%, 4/9) (Figure 1B).

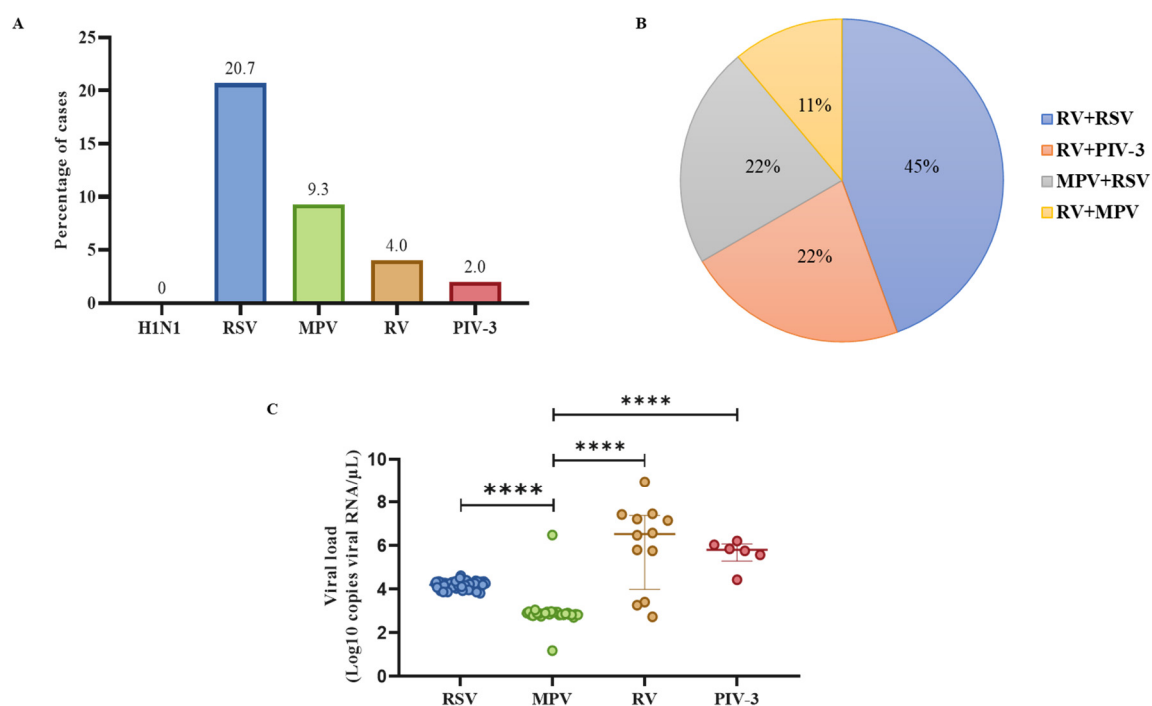


Figure 1. Circulation, dual co-infections, and viral load of non-SARS-CoV-2 respiratory viruses in population with ARIs in the south of Mexico. (A) Frequency of non-SARS-CoV-2 respiratory viruses in the population with ARIs. (B) Dual co-infections detected in the population with ARIs negative for SARS-CoV-2. (C) Comparison of viral loads of samples positive for RSV, MPV, RV, and PIV-3 infection. The data were analyzed with the Kruskal–Wallis test, followed by a multiple comparison analysis of Dunnett's, **** $p < 0.0001$. Abbreviations: H1N1, Influenza A H1N1; RSV, respiratory syncytial virus; MPV, metapneumovirus; RV, rhinovirus; PIV-3, parainfluenza virus-3.

3.2. Patients positive for RV infection had the highest viral loads compared to other respiratory viruses

To compare viral loads among samples positive for RSV, MPV, RV, and PIV-3, absolute quantification of the viral genome copies was performed using RT-qPCR and the standard curves specific for each virus. The highest viral loads were found in the samples positive for RV, while the lowest viral loads were associated with MPV infection. Multiple comparative analyses showed significant differences between the viral loads of MPV and those of RSV, RV, and PIV-3 (Figure 1C).

3.3. Single infection or dual co-infection with non-SARS-CoV-2 viruses was characterized by an increase in the expression of IL-1RA and MIP-1 α

To determine the level of expression of cytokines and chemokines in the population with IRAs associated with VSR, MPV, RV, and PIV-3 infections, a multiplex immunoassay was performed for the detection of 27 cytokines. The panel of cytokines was classified into three groups according to the type of immune response they coordinate: proinflammatory (FGF basic, G-CSF, GM-CSF, IL-1 β , IL-2, IL-6, IL-7, IL-12p70, IL-15, IL-17A, IFN- γ , TNF- α , and VEGF), anti-inflammatory (IL-1RA, IL-4, IL-5, IL-6, IL-9, IL-10, IL-13, and PDGF-BB) and chemotaxis (Eotaxin, IL-8, IP-10, MCP-1, MIP-1 α , MIP-1 β , and RANTES).

Of the 27 cytokines analyzed, IL-RA and MIP-1 α were the only ones that exhibited increased protein expression levels in single infections and dual co-infections compared to the controls. The other cytokines showed differential expression. IL-1 β , IL-4, IL-7, IL-12p70, IL-13, and TNF- α were not detected in the healthy controls or single infections, except TNF α , induced by RSV, and MCP-1 α , induced by MPV and RV (Table 1).

The proinflammatory cytokines MIP-1 β , MCP-1, IL-8, and IP-10 were upregulated in common during infection by RV and MPV, while RSV increased levels of RANTES, MIP-1 β , and, as mentioned, TNF α . Interestingly, the immunomodulatory IL-1RA was only augmented by RSV and RV in single infections. In agreement with such results, we observed increased levels of IL-1RA during co-infection with RV associated with RSV or PIV3. In addition, the pair RV+RSV induced a more diverse expression of inflammatory cytokines (IL-8, IL-9, IL-15, IL-17A, MCP-1, MIP-1 α , MIP-1 β , PDGF-BB, RANTES, and VEGF) than the other virus pairs (Table 2).

Table 1. Cytokine levels (pg/mL) in patients positive for single RSV, MPV, RV, and PIV-3 infection.

| Cytokine | Controls | | | RSV | | | MPV | | | RV | | | PIV-3 | | |
|----------------|----------|--------|------------------|-----|--------|------------------|-----|--------|------------------|----|---------|------------------|-------|--------|------------------|
| | n | Median | Percentile 25-75 | n | Median | Percentile 25-75 | n | Median | Percentile 25-75 | n | Median | Percentile 25-75 | n | Median | Percentile 25-75 |
| Eotaxin | 3 | 0.63 | 0.18-1.11 | 5 | 1.05 | 0.50-1.40 | 5 | 0.75 | 0.32-1.01 | 4 | 0.67 | 0.5-2.09 | 3 | 0 | 0-0.72 |
| FGF basic | 3 | 25.9 | 0-29.73 | 5 | 15.405 | 14.19-37.73 | 5 | 14.19 | 0-16.56 | 4 | 7.40 | 1.66-16.55 | 3 | 0 | 0-17.66 |
| G-CSF | 3 | 425.72 | 201.56-830.91 | 5 | 223.83 | 196.29-341.91 | 5 | 472.28 | 432.48-645.06 | 4 | 1144.28 | 782.8-2624.34 | 3 | 239.43 | 55.5-1486.55 |
| GM-CSF | 3 | 6.78 | 0-7.7 | 5 | 5.03 | 0-9.83 | 5 | 2.37 | 0-8.91 | 4 | 2.87 | 1.12-4.56 | 3 | 0 | 0-3.26 |
| IL-1 β | 3 | 0.00 | 0-0.57 | 5 | 0.18 | 0-0.57 | 5 | 0 | 0-0.57 | 4 | 0.23 | 0-0.51 | 3 | 0 | 0-0.03 |
| IL-1RA | 3 | 14.28 | 0-14.28 | 5 | 77.39 | 57.18-155.06 | 5 | 14.28 | 0-160.01 | 4 | 38.03 | 16.95-49.67 | 3 | 14.28 | 0-64.17 |
| IL-2 | 3 | 6.12 | 2.9-8.19 | 5 | 2.39 | 1.23-11.30 | 5 | 4.46 | 4.05-4.67 | 4 | 2.49 | 2.28-2.90 | 3 | 1.65 | 0-3.95 |
| IL-4 | 3 | 0.00 | 0-0 | 5 | 0.00 | 0-0 | 5 | 0 | 0-0 | 4 | 0 | 0-0 | 3 | 0 | 0-1.89 |
| IL-5 | 3 | 27.57 | 0-31.67 | 5 | 0.00 | 0-2.39 | 5 | 0 | 0-23.42 | 4 | 0.26 | 0-11.62 | 3 | 0 | 0-5.73 |
| IL-6 | 3 | 2.45 | 0.51-2.61 | 5 | 2.09 | 0-4.71 | 5 | 1.28 | 0.42-1.65 | 4 | 0.52 | 0.16-0.91 | 3 | 0 | 0-1.82 |
| IL-7 | 3 | 0.00 | 0-0 | 5 | 0 | 0-0 | 5 | 0 | 0-0 | 4 | 0 | 0-0 | 3 | 0 | 0-0 |
| IL-8 | 3 | 3.92 | 2.7-5.73 | 5 | 6.33 | 3.11-9.77 | 5 | 14.22 | 6.03-18.27 | 4 | 28.21 | 8.27-171.76 | 3 | 2.81 | 0-3.3 |
| IL-9 | 3 | 9.00 | 7.65-10.52 | 5 | 8.33 | 6.96-10.68 | 5 | 7.98 | 5.76-9.33 | 4 | 7.30 | 5.06-8.49 | 3 | 13.35 | 7.98-34.29 |
| IL-10 | 3 | 1.82 | 0.03-2.09 | 5 | 1.67 | 0-2.36 | 5 | 1.40 | 0.51-1.53 | 4 | 2.36 | 1.66-2.36 | 3 | 0.96 | 0-1.53 |
| IL-12p70 | 3 | 0.00 | 0-2.33 | 5 | 0.00 | 0-0 | 5 | 0 | 0-0 | 4 | 0 | 0-0 | 3 | 0 | 0-0 |
| IL-13 | 3 | 0.00 | 0-0 | 5 | 0.00 | 0-1.22 | 5 | 0.45 | 0.32-0.56 | 4 | 0 | 0-0.3 | 3 | 0 | 0-0.78 |
| IL-15 | 3 | 333.08 | 222.98-449.64 | 5 | 194.16 | 0-260.6 | 5 | 242.48 | 242.48-248.66 | 4 | 211.26 | 86.93-271.18 | 3 | 111.71 | 0-372.8 |
| IL-17A | 3 | 12.09 | 9.98-12.8 | 5 | 6.62 | 0.33-8.06 | 5 | 13.74 | 11.16-18.36 | 4 | 5.38 | 3.39-7.46 | 3 | 6.12 | 0-7.1 |
| IFN- γ | 3 | 2.66 | 0-3.05 | 5 | 3.23 | 1.74-3.33 | 5 | 2.66 | 2.06-3.96 | 4 | 2.56 | 2.36-2.66 | 3 | 2.16 | 0.14-6.2 |
| IP-10 | 3 | 18.08 | 0-22.07 | 5 | 5.24 | 0-8.49 | 5 | 25.49 | 12.3-268.52 | 4 | 314.85 | 185.39-437.22 | 3 | 0 | 0-10.59 |
| MCP-1 | 3 | 0.83 | 0-3.48 | 5 | 2.13 | 0-3.48 | 5 | 6.14 | 5.75-6.14 | 4 | 15.02 | 5.93-24.46 | 3 | 0.83 | 0-0.83 |
| MIP-1 α | 3 | 0.45 | 0-0.62 | 5 | 1.31 | 1.31-1.58 | 5 | 0.98 | 0.84-1.31 | 4 | 1.97 | 1.43-9.16 | 3 | 1.35 | 0.71-1.35 |

| | | | | | | | | | | | | | | | |
|---------------|---|--------|---------------|---|-------|-------------|---|-------|-------------|---|-------|--------------|---|-------|-----------|
| MIP-1 β | 3 | 6.89 | 3.78-14.51 | 5 | 14.18 | 7.73-15.83 | 5 | 23.21 | 8.63-23.91 | 4 | 52.17 | 36.61-187.19 | 3 | 2.79 | 0-17.61 |
| PDGF-BB | 3 | 40.26 | 18.72-54.24 | 5 | 39.45 | 26.88-52.73 | 5 | 25.73 | 19.65-30.35 | 4 | 59.45 | 38.45-68.84 | 3 | 21.51 | 0-40.26 |
| RANTES | 3 | 9.51 | 4.59-10.73 | 5 | 15.12 | 5.1-16.53 | 5 | 13.59 | 10.73-13.94 | 4 | 8.60 | 5.50-16.73 | 3 | 6.09 | 1.37-7.44 |
| TNF- α | 3 | 0.00 | 0-0 | 5 | 7.05 | 0-12.47 | 5 | 0 | 0-1.70 | 4 | 0.85 | 0-2.12 | 3 | 0 | 0-0 |
| VEGF | 3 | 377.79 | 187.52-589.74 | 5 | 0 | 0-0 | 5 | 0 | 0-0 | 4 | 43.46 | 0-90.29 | 3 | 0 | 0-245.75 |

The *n* represents the number of samples in which the cytokines were analyzed for each condition. Abbreviations: FGF basic, fibroblast growth factor basic; G-CSF, granulocyte colony-stimulating factor; GM-CSF, granulocyte-macrophage colony-stimulating factor; IL, interleukin; RA, receptor antagonist; IFN, interferon; IP-10, IFN- γ inducible protein-10; MCP-1, monocyte chemoattractant protein-1, MIP, macrophage-inflammatory protein; PDGF-BB, platelet-derived growth factor-BB; RANTES, regulated upon activation normal T cell expressed and secreted; TNF, tumor necrosis factor; VEGF: vascular endothelial growth factor.

Table 2. Cytokine levels (pg/mL) in patients positive for non-SARS-CoV-2 respiratory viruses dual co-infection.

| Cytokine | RV+RSV | | | RV+PIV-3 | | | MPV+RSV | | | RV+MPV | | |
|--------------|--------|--------|------------------|----------|--------|------------------|---------|--------|------------------|--------|---------|------------------|
| | n | Median | Percentile 25-75 | n | Median | Percentile 25-75 | n | Median | Percentile 25-75 | n | Median | Percentile 25-75 |
| Eotaxin | 4 | 1.43 | 0.7-2 | 2 | 0.4 | 0.11-0.69 | 2 | 0.44 | 0-0.89 | 1 | 0 | --- |
| FGF basic | 4 | 7.7 | 0-62.17 | 2 | 0 | 0-0 | 2 | 0 | 0-0 | 1 | 0 | --- |
| G-CSF | 4 | 1035.1 | 394.4-1808.09 | 2 | 262.81 | 110.99-414.63 | 2 | 134.41 | 119.33-149.49 | 1 | 3655.38 | --- |
| GM-CSF | 4 | 4.47 | 0.19-8.65 | 2 | 1.12 | 0-2.24 | 2 | 11.69 | 4.4-18.98 | 1 | 0 | --- |
| IL-1 β | 4 | 0 | 0-0.38 | 2 | 0 | 0-0 | 2 | 0 | 0-0 | 1 | 0 | --- |
| IL-1RA | 4 | 75.03 | 0-228.37 | 2 | 96.96 | 33.9-160.01 | 2 | 0 | 0-0 | 1 | 0 | --- |
| IL-2 | 4 | 2.64 | 1.34-5.3 | 2 | 0 | 0-0 | 2 | 1.39 | 0.81-1.97 | 1 | 0 | --- |
| IL-4 | 4 | 0.18 | 0-0.5 | 2 | 0.71 | 0-1.41 | 2 | 0.29 | 0-0.59 | 1 | 0 | --- |
| IL-5 | 4 | 2.05 | 0-32.57 | 2 | 0 | 0-0 | 2 | 0 | 0-0 | 1 | 0 | --- |
| IL-6 | 4 | 0.16 | 0-0.98 | 2 | 1.22 | 0-2.45 | 2 | 0 | 0-0 | 1 | 20.7 | --- |
| IL-7 | 4 | 0 | 0-9.72 | 2 | 0 | 0-0 | 2 | 1.26 | 0-2.52 | 1 | 0 | --- |
| IL-8 | 4 | 42.25 | 22.43-205.58 | 2 | 12.43 | 0-24.86 | 2 | 3.37 | 0-6.74 | 1 | 6.84 | --- |
| IL-9 | 4 | 11.44 | 3.45-17.3 | 2 | 9.77 | 4.55-15 | 2 | 5.58 | 4.55-6.62 | 1 | 4.02 | --- |
| IL-10 | 4 | 1.1 | 0.33-5.3 | 2 | 0 | 0-0 | 2 | 0.55 | 0-1.1 | 1 | 0 | --- |

| | | | | | | | | | | | | |
|----------------|---|--------|----------------|---|-------|-----------|---|--------|-------------|---|--------|-----|
| IL-12p70 | 4 | 0 | 0-2.48 | 2 | 0 | 0-0 | 2 | 0 | 0-0 | 1 | 0 | --- |
| IL-13 | 4 | 0.82 | 0-2.12 | 2 | 0.39 | 0-0.78 | 2 | 0.74 | 0-1.49 | 1 | 0 | --- |
| IL-15 | 4 | 151.46 | 97.45-252.24 | 2 | 52.47 | 0-104.94 | 2 | 238.63 | 0-477.26 | 1 | 0 | --- |
| IL-17A | 4 | 15.86 | 2.94-32.295 | 2 | 1.17 | 0.5-1.85 | 2 | 9.36 | 6.86-11.87 | 1 | 2.1 | --- |
| IFN- γ | 4 | 1.19 | 0.32-4.22 | 2 | 3.29 | 1.4-5.19 | 2 | 0.92 | 0-1.85 | 1 | 0 | --- |
| IP-10 | 4 | 415.38 | 145.83-2349.82 | 2 | 3.79 | 0-7.58 | 2 | 27.11 | 0-54.21 | 1 | 418.28 | --- |
| MCP-1 | 4 | 24.53 | 7.64-71.65 | 2 | 1.67 | 0-3.33 | 2 | 7.57 | 3.17-11.97 | 1 | 16.1 | --- |
| MIP-1 α | 4 | 7.83 | 0.7-16.7 | 2 | 0.96 | 0.53-1.4 | 2 | 0.49 | 0-0.98 | 1 | 1.2 | --- |
| MIP-1 β | 4 | 56.27 | 11.84-153.4 | 2 | 4.59 | 3.96-5.22 | 2 | 2.54 | 1.29-3.78 | 1 | 27.83 | --- |
| PDGF-BB | 4 | 25.97 | 11.66-45.14 | 2 | 0 | 0-0 | 2 | 29.57 | 11.78-47.36 | 1 | 0 | --- |
| RANTES | 4 | 11.86 | 8.48-61.88 | 2 | 4.21 | 2.82-5.6 | 2 | 4.34 | 3.59-5.1 | 1 | 0 | --- |
| TNF- α | 4 | 4.57 | 0-16.08 | 2 | 0 | 0-0 | 2 | 3.53 | 0-7.05 | 1 | 13.76 | --- |
| VEGF | 4 | 88.40 | 0-201.26 | 2 | 14.02 | 0-28.04 | 2 | 50.06 | 0-100.13 | 1 | 0 | --- |

The *n* represents the number of samples in which the cytokines were analyzed for each condition. Abbreviations: FGF basic, fibroblast growth factor basic; G-CSF, granulocyte colony-stimulating factor; GM-CSF, granulocyte-macrophage colony-stimulating factor; IL, interleukin; RA, receptor antagonist; IFN, interferon; IP-10, IFN- γ inducible protein-10; MCP-1, monocyte chemoattractant protein-1, MIP, macrophage-inflammatory protein; PDGF-BB, platelet-derived growth factor-BB; RANTES, regulated upon activation normal T cell expressed and secreted; TNF, tumor necrosis factor; VEGF: vascular endothelial growth factor.

3.4. G-CSF, IP-10, and VEGF expression were decreased in PIV-3 dual co-infections. FGF basic, MIP-1 α , IL-8, IP-10, MCP-1, IFN- γ , and RANTES are differentially expressed between single infections and dual co-infections

To investigate whether the differential expression of these cytokines is a hallmark of non-SARS-CoV-2 virus infection, samples from patients with single SARS-CoV-2 infection and SARS-CoV-2+PIV-3 co-infection patients were analyzed. SARS-CoV-2-positive samples did not show expressions of IL-1 β , IL-4, IL-7, IL-13, TNF- α , or IL-12p70. Of the cytokines detected, G-CSF, IP-10, and VEGF showed higher concentrations in single infection than in co-infection. In contrast, IL-1RA, IL-15, MIP-1 β , and PDGF-BB were found at lower levels in single SARS-CoV-2 infection. Also, PIV-3, in co-infection with SARS-CoV-2 or RV, showed lower levels of G-CSF, IL-17A, RANTES, and VEGF in common with respect to the controls, suggesting that changes in the expressions of these cytokines may be regulated by PIV-3, and this co-infection might be of low risk to develop severe illness [41] (Table 3).

Table 3. Cytokine levels (pg/mL) in patients positive for single SARS-CoV-2 infection and dual co-infection.

| Cytokine | SARS-CoV-2 | | | SARS-CoV-2+PIV-3 | | |
|----------------|------------|--------|------------------|------------------|--------|------------------|
| | n | Median | Percentile 25-75 | n | Median | Percentile 25-75 |
| Eotaxin | 6 | 0.44 | 0.24-0.72 | 2 | 0.74 | 0.24-1.25 |
| FGF basic | 6 | 0 | 0-0 | 2 | 12.13 | 0-24.26 |
| G-CSF | 6 | 741.42 | 116.55-2274.51 | 2 | 269.42 | 136.55-402.29 |
| GM-CSF | 6 | 0 | 0-0 | 2 | 3.11 | 0-6.21 |
| IL-1 β | 6 | 0 | 0-0.63 | 2 | 0 | 0-0 |
| IL-1RA | 6 | 32.09 | 0-89.82 | 2 | 49.88 | 49.88-49.88 |
| IL-2 | 6 | 4.1 | 1.76-5.91 | 2 | 2.59 | 1.76-3.42 |
| IL-4 | 6 | 0 | 0-0 | 2 | 0 | 0-0 |
| IL-5 | 6 | 3.26 | 0-25.5 | 2 | 6.77 | 2.39-11.16 |
| IL-6 | 6 | 0 | 0-0 | 2 | 1.55 | 1.1-2 |
| IL-7 | 6 | 0 | 0-0 | 2 | 0 | 0-0 |
| IL-8 | 6 | 3.71 | 3.11-8.36 | 2 | 1.65 | 0-3.3 |
| IL-9 | 6 | 4.36 | 0.95-11.69 | 2 | 5.93 | 5.24-6.62 |
| IL-10 | 6 | 0 | 0-1.82 | 2 | 0.95 | 0.66-1.25 |
| IL-12p70 | 6 | 0 | 0-0 | 2 | 0 | 0-0 |
| IL-13 | 6 | 0 | 0-0 | 2 | 0.16 | 0-0.32 |
| IL-15 | 6 | 237.33 | 0-328.4 | 2 | 298.72 | 288.42-309.02 |
| IL-17A | 6 | 1.95 | 0-14.21 | 2 | 3.71 | 1.05-6.36 |
| IFN- γ | 6 | 0.85 | 0.0-1.4 | 2 | 2.84 | 1.62-4.05 |
| IP-10 | 6 | 203.91 | 128.09-240.17 | 2 | 121.76 | 0.83-242.7 |
| MCP-1 | 6 | 6.56 | 0-14.75 | 2 | 4.28 | 0.15-8.4 |
| MIP-1 α | 6 | 0.84 | 0-1.67 | 2 | 1.52 | 0.98-2.07 |
| MIP-1 β | 6 | 17.08 | 7.65-29.54 | 2 | 21.38 | 1.19-41.57 |
| PDGF-BB | 6 | 18.7 | 0-45.8 | 2 | 24.48 | 17.76-31.2 |
| RANTES | 6 | 3.26 | 0.96-5.34 | 2 | 6.08 | 4.35-7.82 |

| | | | | | | |
|---------------|---|--------|---------|---|--------|---------------|
| TNF- α | 6 | 0 | 0-9.81 | 2 | 0.4 | 0-0.8 |
| VEGF | 6 | 274.63 | 0-414.8 | 2 | 212.45 | 194.46-230.43 |

The *n* represents the number of samples in which the cytokines were analyzed for each condition. Abbreviations: FGF basic, fibroblast growth factor basic; G-CSF, granulocyte colony-stimulating factor; GM-CSF, granulocyte-macrophage colony-stimulating factor; IL, Interleukin; RA, receptor antagonist; IFN, interferon; IP-10, IFN- γ inducible protein-10; MCP-1, monocyte chemoattractant protein-1, MIP, macrophage-inflammatory protein; PDGF-BB, platelet-derived growth factor-BB; RANTES, regulated upon activation normal T cell expressed and secreted; TNF, tumor necrosis factor; VEGF: vascular endothelial growth factor.

On the other hand, to establish the profiles of the inflammatory and antiviral immune response during single RSV, RV, MPV, and PIV-3 infection and most frequent viral dual co-infections, the concentrations of each of the cytokines and chemokines were transformed and expressed as Log₁₀ and are represented in a radar chart. Concentrations outside the detection range were arbitrarily replaced at 0. The general patterns of cytokine expression between the single infections and dual co-infections were markedly characterized by the induction of IL-1RA. However, in the MPV dual co-infections, this anti-inflammatory cytokine was not detected.

As for the cytokines and chemokines expressed differentially in single infections and dual co-infections, RV+RSV co-infection was characterized by high levels of expression of FGF basic ($p>0.99$) and MIP-1 α ($p=0.23$). The cases of single RV infection and RV+RSV co-infection showed a marked increase in the expressions of IL-8 and IP-10 compared to the controls and other infections or dual co-infections. Single PIV-3 infection was characterized by decreased levels of MCP-1 ($p>0.99$) compared to those infected with one or two viruses and the controls. Single RSV infection was a unique viral infection characterized by an increase in IFN- γ expression compared to the controls. On the other hand, RV+RSV co-infection was a unique dual co-infection in which a marked increase in RANTES expression was observed (Figure 2A-2C). Together, these results suggest a distinctive signature of the SARS-CoV-2 infection and non-SARS-CoV-2 viruses.

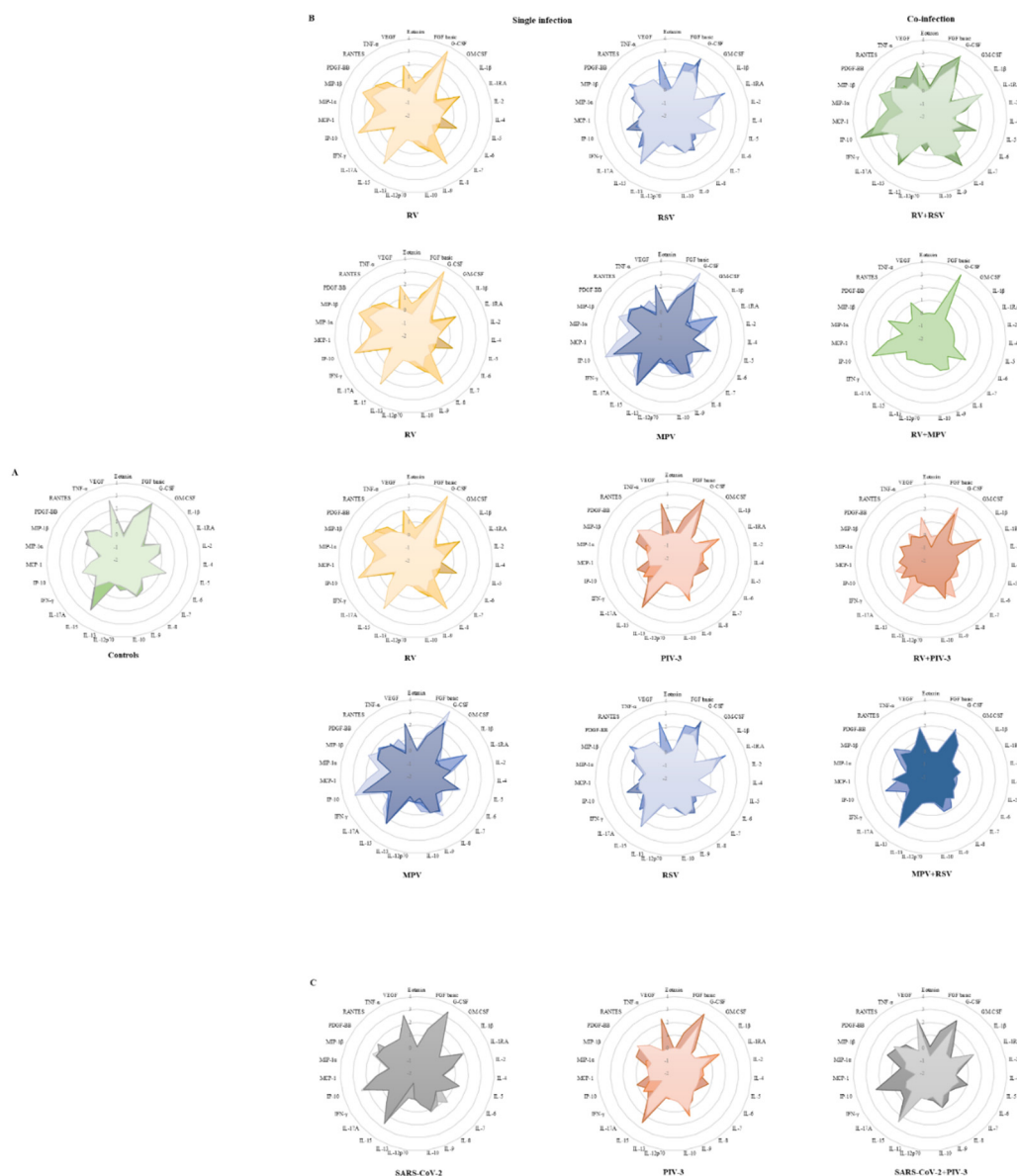


Figure 2. Comparison of expression profiles of cytokines in healthy individuals and single infection and dual co-infection with RSV, MPV, RV, PIV-3, and SARS-CoV-2. (A) Log₁₀ of the concentration values of the cytokines and chemokines in controls, (B) single infection and dual co-infection with non-SARS-CoV-2 viruses, and (C) SARS-CoV-2 virus. Each radar chart accounts for the 27 cytokines assessed in each viral infection. Concentrations outside the detection range were established at 0. Abbreviations: FGF basic, fibroblast growth factor basic; G-CSF, granulocyte colony-stimulating factor; GM-CSF, granulocyte-macrophage colony-stimulating factor; IL, interleukin; RA, receptor antagonist; IFN, interferon; IP-10, IFN- γ inducible protein-10; MCP-1, monocyte chemoattractant protein-1; MIP, macrophage-inflammatory protein; PDGF-BB, platelet-derived growth factor-BB; RANTES, regulated upon activation normal T cell expressed and secreted; TNF, tumor necrosis factor; VEGF: vascular endothelial growth factor.

3.5. Eotaxin expression levels are significantly associated with RSV viral load

To perform a comparative analysis of the cytokines and chemokines with differential expression, a multiple comparison analysis was performed, and the Spearman correlation coefficient was determined. RV+RSV co-infection was the unique dual co-infection in which increased levels of FGF basic and IL-5 were found, compared to the controls and single infections. Single infection with the highest viral load (RV) showed lower levels of IFN- γ expression than the controls ($p=0.83$), while single infection with a lower viral load (RSV), showed the most increased levels ($p=0.40$). On the other

hand, single SARS-CoV-2 infection was a unique viral infection in which high VEGF levels were found compared to the controls ($p>0.99$) (Figure 3). Single RV infection showed increased levels of PDGF-BB compared to the controls and other single infections or dual co-infections. Single PIV-3 infection and RV+RSV co-infection showed elevated levels of IL-9 compared to the controls and other viral infections ($p>0.99$) (Figure 4). Single PIV-3 infection was a unique viral infection in which decreased levels of MCP-1 were found compared to the controls ($p>0.99$). RV+RSV co-infection was a unique dual infection that induced high expressions of IL-8 and MIP-1 α compared to the controls and single infection cases (Figure 5). Significant differences were observed between the expression levels of Eotaxin and the viral load of RSV ($p=0.03$) (Supplementary Table 4).

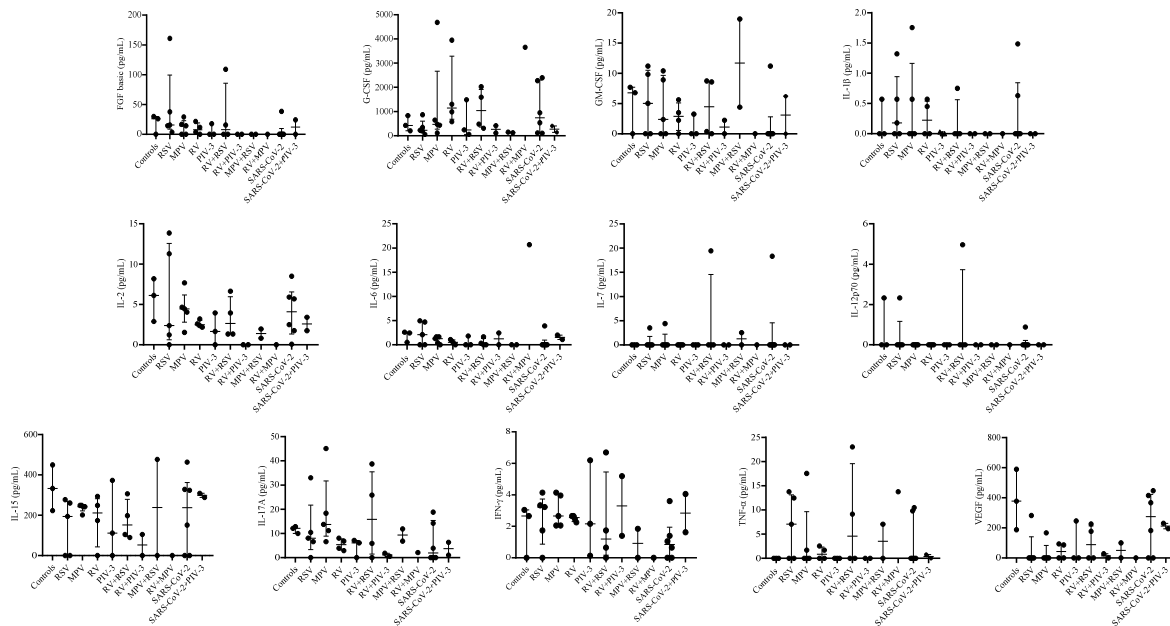


Figure 3. Expression of pro-inflammatory cytokines in single infection and dual co-infection with RSV, MPV, RV, PIV-3, and SARS-CoV-2. Data are expressed as median with range or median with 25th and 75th percentiles. One-way ANOVA was applied to normally distributed data, followed by Dunnett's multiple comparison test. Kruskal–Wallis test was applied to the rest, followed by Dunn's multiple comparison test. No detectable levels of IL-1 β , IL-7, or IL-12p70 were found in SARS-CoV-2+PIV-3 co-infection. Abbreviations: FGF basic, fibroblast growth factor basic; G-CSF, granulocyte colony-stimulating factor; GM-CSF, granulocyte–macrophage colony-stimulating factor; IL, interleukin; IPN, interferon; TNF, tumor necrosis factor; VEGF, vascular endothelial growth factor.

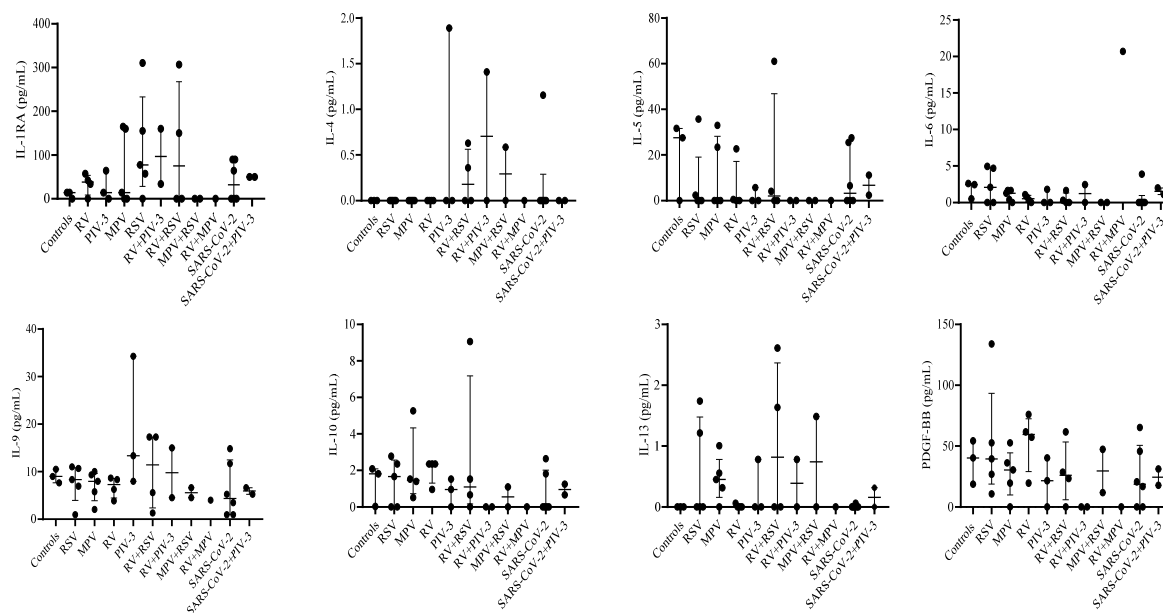


Figure 4. Expression of anti-inflammatory cytokines in single infection and dual co-infection with RSV, MPV, RV, PIV-3, and SARS-CoV-2. Data are expressed as median with 25th and 75th percentiles and analyzed with the Kruskal–Wallis test, followed by Dunn’s multiple comparison test. No detectable levels of IL-4 were found in SARS-CoV-2+PIV-3 co-infection. Abbreviations: IL, interleukin; RA, receptor antagonist; PDGF-BB, platelet-derived growth factor-BB.

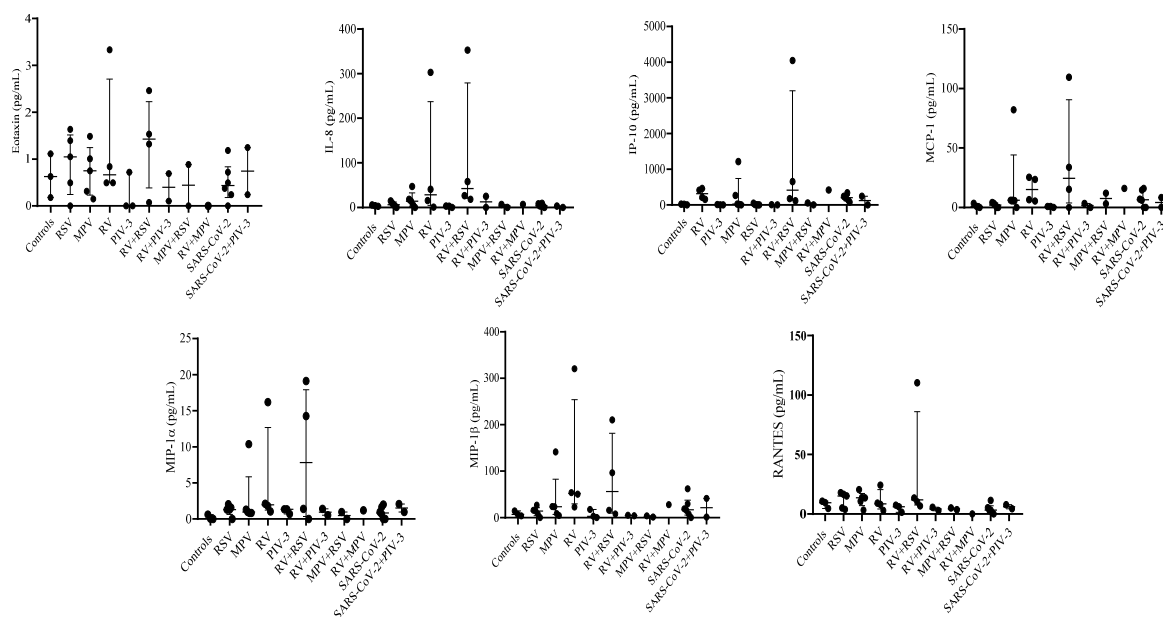


Figure 5. Expression of chemokines in single infection and dual co-infection with RSV, MPV, RV, PIV-3, and SARS-CoV-2. Data are expressed as median with 25th and 75th percentiles and analyzed with the Kruskal–Wallis test, followed by Dunn’s multiple comparison test. Abbreviations: MCP-1, monocyte chemoattractant protein-1; IP-10, IFN- γ inducible protein-1; MIP, macrophage-inflammatory protein; RANTES, regulated upon activation normal T cell expressed and secreted.

4. Discussion

IRAs caused by RNA respiratory viruses are the most frequent causes of hospital admission, which reached the highest rate during the COVID-19 pandemic. However, there is little information about the epidemiology of RNA viruses that circulated during the COVID-19 pandemic and patterns

of infection associated with feasible co-infections and the immune response. Herein, we studied four of the most relevant non-SARS-CoV-2 viruses related not only to upper but also to lower respiratory tract disease in a group of children and adults with ARI. RSV was the main etiology of ARI, indicating it remains one of the most important respiratory viruses, in agreement with previous studies that reported RSV infecting both children and adults, highlighting its importance at all ages [12]. It is well known that many respiratory viruses show enhanced spread in winter months, indicating that lower temperatures and social behavior improve transmission, [4] determining seasonality [42].

Global RSV epidemics start in the Southern Hemisphere and move to the Northern Hemisphere. In most countries in the Southern Hemisphere, RSV epidemics started between March and June, and in countries in the Northern Hemisphere, between September and December [43], with higher incidence during winter [5]. However, it is clear that the COVID-19 pandemic not only altered RSV circulation across geographic regions, climate zones, and at-risk groups [44–46], but also affected the seasonality pattern since our recovery of RSV-positive samples occurred between January and March, with a higher peak in the first week of February (Supplementary Figure 1).

In the same period, ARI was associated with infections of MPV (9.3%), RV (4.0%), and PIV-3 (2.0%). Normally, MPV and RV are detected throughout the year [4], whereas PIV epidemics are mainly detected in the spring and early summer [47]. The PIV-3 cases reported in our study were detected during the winter, suggesting that its pattern of circulation was also altered. Interestingly, we did not find positive cases of Influenza A H1N1. The most probable explanation for the disappearance of influenza in the South of Mexico and changes in the pattern of circulation of the other viruses are a consequence of the implemented strategies to reduce SARS-CoV-2 transmission, such as physical distancing, the use of face masks, frequent hand washing, and the isolation of individuals with respiratory symptoms, as previously reported [48].

Most patients positive for the viruses of interest showed single infections (91.7%), whereas co-infections with two viruses displayed low frequency (8.3%). RV was the most common virus in co-infections, and the most frequent of those was RV+RSV. Our results coincide with those of a study that reported that viral co-infections principally involve RV and RSV [49]. Another study reported that RSV is frequently found in co-infection with bacteria [50] as *Staphylococcus aureus*, *Pseudomonas aeruginosa*, *Streptococcus pneumoniae*, *Moraxella catarrhalis*, *Haemophilus influenzae*, and *Klebsiella pneumoniae* [51]. In our study, we do not exclude the possibility that the group studied could have had a bacterial infection, as respective molecular detection was not performed.

We determined the viral loads using nasopharyngeal swabs, and we found that positive patients for RV had the highest viral load, whereas positive patients for MPV showed the lowest viral loads compared to the other viruses studied ($p < 0.0001$). It has been reported that in adults, the high viral load of RV is associated with symptom severity but not with symptom duration [52]. In contrast, a study reported that, in children, the viral load of MPV is significantly correlated with the course of illness, finding high viral loads in those who had it for 6 to 11 days compared to those who had it for less than 5 days or more than 11 days, suggesting that the viral load of MPV is significantly correlated with the course of illness and that between days 6 and 11, high MPV viral shedding occurs [53]. We consider that nasopharyngeal swabs were an appropriate sample for virus detection and viral load quantification. However, an important limitation of our study is that we do not know on which day of the course of illness the samples were taken; in addition, we do not have the clinical data of the patients' oxygen saturation. Therefore, we suggest that the course of illness can be an important factor in the context of the viral load and highlight the importance of sampling from the beginning of the symptoms.

In our study, we also found that, in 71% of RV dual co-infections, the RV viral load was higher than that of the other co-infecting viruses (Supplementary Table 5). This finding could be explained by a study that described that, in viral co-infections, a virus competitively suppresses the replication of another, which is termed viral interference [54]. Interestingly, a mathematical model showed that during co-infections, a fast-growing virus could block a slow-growing virus simply by being the first that started infection, consuming more target cells without immediate viral interference by immune response. This study showed that RV is the fastest-growing virus and reduces replication of the other

viruses (PIV, MPV, RSV, and influenza A) during co-infection, while RSV has the slowest-growing rate with longer infecting times than the other viruses, and its replication is suppressed in the presence of other viruses [55]. Although we did not determine the viral load of SARS-CoV-2, a study found that the replication of this virus is easily suppressed by other respiratory viruses during co-infection. That study also showed that despite the fact that SARS-CoV-2 replication was largely suppressed, co-infections will be detected since the SARS-CoV-2 viral load is high and decays slowly [56].

Surprisingly, we found that the single infection with the highest viral load (RV) showed lower levels of IFN- γ expression than the controls, while single infection with a lower viral load (RSV) showed increased levels of this cytokine. In contrast to our results, a study showed that, in infants, RSV infection, compared to RV infection and other respiratory viruses, was associated with lower IFN- γ production [57]. On the other hand, another study showed significantly lower IFN- γ levels in nasopharyngeal aspirates from RSV-infected patients compared to MPV-infected patients, suggesting the suppression of host IFN- γ -production by NS1 and NS2 proteins of RSV, through the suppressor of cytokine signaling (SOCS) proteins and IFN-stimulated gene-15 (ISG15) proteins, could play an important role [58]. We consider that an increased expression of IFN- γ in response to RSV infection could be associated with clinical and viral variables, the nasopharyngeal airway microbiome, and metabolome, as previously demonstrated [59].

Cytokine and chemokine expression profiles in patients positive for single infections and co-infections of non-SARS-CoV-2 viruses exhibited increased levels of the immunoregulatory IL-1RA compared to the controls, suggesting their participation in controlling inflammation. FGF basic, IL-8, IP-10, MCP-1, MIP-1 α , IFN- γ , and RANTES were differentially expressed. We also found decreased expressions of G-CSF and VEGF in PIV-3 dual co-infections but not in single SARS-CoV-2 infections. This finding could be consistent with an inflammatory phenotype in patients with COVID-19 with notoriously elevated cytokines, such as G-CSF [60]. We hypothesize that PIV-3 co-infections could have a protective effect on the cytokine response (Figure 5B-5C) and a milder form of the infection. We consider that, even though host response depends on the viral load, also the infection time course, age, and sex may contribute to disease severity, as demonstrated in another study [61]. IL-8 and MIP-1 α were chemokines with the highest expression in RV+RSV co-infection compared to the controls and those infected with one virus. Another important finding was that RV+RSV co-infection was the unique dual co-infection in which a marked increase in RANTES expression was found. In addition, significant differences were observed between the expression levels of eotaxin and the viral load of RSV ($p=0.03$). We hypothesized that differences in the eotaxin expression could be involved in immunity cell responses in individuals infected with RSV [62]. In this work, we report, for the first time, the circulation of RSV, MPV, RV, and PIV-3 in the south of Mexico during the COVID-19 pandemic and the cytokine and chemokine profiles associated with these viral infections and co-infections. We suggest that, together, these inflammatory biomarkers could have significant diagnostic value in the respiratory illness caused by non-SARS-CoV-2 viruses.

5. Conclusions

The emergence of SARS-CoV-2 decreased the circulation of non-SARS-CoV-2 respiratory viruses in the world. In the first year of the pandemic, laboratories prioritized diagnostics for COVID-19, reducing the diagnosis for other respiratory viruses, which cause infections with similar clinical manifestations. Therefore, the circulation and co-circulation of other respiratory viruses during the COVID-19 pandemic could have aggravated many cases. Our study showed that although non-pharmaceutical interventions to reduce the transmission of SARS-CoV-2 were intensified, other respiratory viruses were still circulating, although at a slower rate. We found that the cytokine and chemokine expression profiles were different between single virus infections and dual co-infections. The determination of cytokine and chemokine expression in nasopharyngeal swabs provides reliable information about the local immune response to viral infections. Considering the relatively small sample size of patients with IRAs negative for SARS-CoV-2 in our study, external validation is

warranted. We consider it important to investigate the behavior of circulating respiratory viruses in the presence of a new pandemic-causing virus.

Supplementary Materials: The following supporting information can be downloaded at the website of this paper posted on Preprints.org. Supplementary Table 1: Clinical characteristics of the population in the south of Mexico with ARIs negative for SARS-CoV-2; Supplementary Table 2: Co-morbidities of the population in the south of Mexico with ARIs negative for SARS-CoV-2; Supplementary Table 3: Nucleotide sequences of primers and probes used for real-time TaqMan PCR; Supplementary Table 4: Correlations between cytokine concentration (pg/mL) and viral load (Log₁₀ copies viral RNA/μL); Supplementary Table 5: Viral load of samples positive for non-SARS-CoV-2 respiratory virus co-infection; Supplementary Figure 1: Cumulative non-SARS-CoV-2 respiratory viruses cases, by epidemiological week, during the COVID-19 pandemic in south of Mexico.

Author Contributions: Conceptualization, B.G.G.-S. and O.D.M.-H.; methodology, B.G.G.-S., F.O.B.-A., D.H.-S., and A.R.-R.; formal analysis, B.G.G.-S., E.R.-T., E.F.-A., J.G.-B., R.A.-A., and O.D.M.-H.; investigation, B.G.G.-S., B.I.-A., and O.D.M.-H.; writing—original draft preparation, B.G.G.-S. and O.D.M.-H.; writing—review & editing, E.R.-T., F.O.B.-A., B.I.-A., E.F.-A., D.H.-S., A.R.-R., J.G.-B., and R.A.-A.; supervision, O.D.M.-H.; project administration, O.D.M.-H.; funding acquisition, O.D.M.-H. All authors have read and agreed to the published version of the manuscript.

Institutional Review Board Statement: All subjects gave their informed consent for inclusion before they participated in the study. The study was conducted in accordance with the Declaration of Helsinki, and approved by the Bioethical Committee of the Universidad Autónoma de Guerrero.

Informed Consent Statement: Informed consent was obtained from all subjects involved in the study.

Acknowledgments: Gómez-Sotelo BG is a doctoral student from Programa de Doctorado en Ciencias Biomédicas, Facultad de Ciencias Químico Biológicas, Universidad Autónoma de Guerrero and received fellowship (CVU 704951) from CONACyT.

Conflicts of Interest: The authors declare no conflict of interest.

References

1. Perin, J.; Mulick, A.; Yeung, D.; Villavicencio, F.; Lopez, G.; Strong, K.L.; Prieto-Merino, D.; Cousens, S.; Black, R.E.; Liu, L. Global, Regional, and National Causes of under-5 Mortality in 2000–19: An Updated Systematic Analysis with Implications for the Sustainable Development Goals. *Lancet Child Adolesc Health* **2022**, *6*, 106–115, doi:10.1016/S2352-4642(21)00311-4.
2. Hodinka, R.L. Respiratory RNA Viruses. *Microbiol Spectr* **2016**, *4*, doi:10.1128/microbiolspec.DMIH2-0028-2016.
3. Price, R.H.M.; Graham, C.; Ramalingam, S. Association between Viral Seasonality and Meteorological Factors. *Sci Rep* **2019**, *9*, 929, doi:10.1038/s41598-018-37481-y.
4. Moriyama, M.; Hugentobler, W.J.; Iwasaki, A. Seasonality of Respiratory Viral Infections. *Annu Rev Virol* **2020**, *7*, 83–101, doi:10.1146/annurev-virology-012420-022445.
5. Audi, A.; Allbrahim, M.; Kaddoura, M.; Hijazi, G.; Yassine, H.M.; Zaraket, H. Seasonality of Respiratory Viral Infections: Will COVID-19 Follow Suit? *Front Public Health* **2020**, *8*, 567184, doi:10.3389/fpubh.2020.567184.
6. Olsen, S.J.; Winn, A.K.; Budd, A.P.; Prill, M.M.; Steel, J.; Midgley, C.M.; Kniss, K.; Burns, E.; Rowe, T.; Foust, A.; et al. Changes in Influenza and Other Respiratory Virus Activity During the COVID-19 Pandemic — United States, 2020–2021. *MMWR Morb Mortal Wkly Rep* **2021**, *70*, 1013–1019, doi:10.15585/mmwr.mm7029a1.
7. Bergeron, H.C.; Tripp, R.A. Immunopathology of RSV: An Updated Review. *Viruses* **2021**, *13*, 2478, doi:10.3390/v13122478.
8. Park, G.Y.S.; Tishkowsky, K. Paramyxovirus. In *StatPearls*; StatPearls Publishing: Treasure Island (FL), 2022.
9. Ali, A.; Lopardo, G.; Scarpellini, B.; Stein, R.T.; Ribeiro, D. Systematic Review on Respiratory Syncytial Virus Epidemiology in Adults and the Elderly in Latin America. *Int J Infect Dis* **2020**, *90*, 170–180, doi:10.1016/j.ijid.2019.10.025.
10. Chadha, M.; Hirve, S.; Bancej, C.; Barr, I.; Baumeister, E.; Caetano, B.; Chittaganpitch, M.; Darmaa, B.; Ellis, J.; Fasce, R.; et al. Human Respiratory Syncytial Virus and Influenza Seasonality Patterns—Early Findings

- from the WHO Global Respiratory Syncytial Virus Surveillance. *Influenza Other Respir Viruses* **2020**, *14*, 638–646, doi:10.1111/irv.12726.
11. Benítez-Guerra, D.; Piña-Flores, C.; Zamora-López, M.; Escalante-Padrón, F.; Lima-Rogel, V.; González-Ortiz, A.M.; Guevara-Tovar, M.; Bernal-Silva, S.; Benito-Cruz, B.; Castillo-Martínez, F.; et al. Respiratory Syncytial Virus Acute Respiratory Infection-Associated Hospitalizations in Preterm Mexican Infants: A Cohort Study. *Influenza Other Respir Viruses* **2020**, *14*, 182–188, doi:10.1111/irv.12708.
 12. Gamiño-Arroyo, A.E.; Moreno-Espinosa, S.; Llamosas-Gallardo, B.; Ortiz-Hernández, A.A.; Guerrero, M.L.; Galindo-Fraga, A.; Galán-Herrera, J.F.; Prado-Galbarro, F.J.; Beigel, J.H.; Ruiz-Palacios, G.M.; et al. Epidemiology and Clinical Characteristics of Respiratory Syncytial Virus Infections among Children and Adults in Mexico. *Influenza Other Respir Viruses* **2017**, *11*, 48–56, doi:10.1111/irv.12414.
 13. Fernandes-Matano, L.; Monroy-Muñoz, I.E.; Uribe-Nogues, L.A.; Hernández-Cueto, M. de L.Á.; Sarquíz-Martínez, B.; Pardavé-Alejandre, H.D.; Coy-Arechavaleta, A.S.; Alvarado-Yaah, J.E.; Rojas-Mendoza, T.; Santacruz-Tinoco, C.E.; et al. [Coinfections by SARS-CoV-2 and other respiratory viruses and their clinical outcome]. *Rev Med Inst Mex Seguro Soc* **2021**, *59*, 482–489.
 14. Noyola, D.E.; Hunsberger, S.; Valdés Salgado, R.; Powers, J.H.; Galindo-Fraga, A.; Ortiz-Hernández, A.A.; Ramirez-Venegas, A.; Moreno-Espinosa, S.; Llamosas-Gallardo, B.; Guerrero, M.L.; et al. Comparison of Rates of Hospitalization Between Single and Dual Virus Detection in a Mexican Cohort of Children and Adults With Influenza-Like Illness. *Open Forum Infect Dis* **2019**, *6*, ofz424, doi:10.1093/ofid/ofz424.
 15. Torres-García, M.; Pérez Méndez, B.B.; Sánchez Huerta, J.L.; Villa Guillén, M.; Rementería Vazquez, V.; Castro Diaz, A.D.; López Martínez, B.; Laris González, A.; Jiménez-Juárez, R.N.; de la Rosa-Zamboni, D. Healthcare-Associated Pneumonia: Don't Forget About Respiratory Viruses! *Front Pediatr* **2019**, *7*, 168, doi:10.3389/fped.2019.00168.
 16. Bochkov, Y.A.; Gern, J.E. Rhinoviruses and Their Receptors: Implications for Allergic Disease. *Curr Allergy Asthma Rep* **2016**, *16*, 30, doi:10.1007/s11882-016-0608-7.
 17. Vandini, S.; Biagi, C.; Fischer, M.; Lanari, M. Impact of Rhinovirus Infections in Children. *Viruses* **2019**, *11*, 521, doi:10.3390/v11060521.
 18. Jackson, D.J.; Gern, J.E. Rhinovirus Infections and Their Roles in Asthma: Etiology and Exacerbations. *The Journal of Allergy and Clinical Immunology: In Practice* **2022**, *10*, 673–681, doi:10.1016/j.jaip.2022.01.006.
 19. Le Glass, E.; Hoang, V.T.; Boschi, C.; Ninove, L.; Zandotti, C.; Boutin, A.; Bremond, V.; Dubourg, G.; Ranque, S.; Lagier, J.-C.; et al. Incidence and Outcome of Coinfections with SARS-CoV-2 and Rhinovirus. *Viruses* **2021**, *13*, 2528, doi:10.3390/v13122528.
 20. Varela, F.H.; Sartor, I.T.S.; Polese-Bonatto, M.; Azevedo, T.R.; Kern, L.B.; Fazolo, T.; de David, C.N.; Zavaglia, G.O.; Fernandes, I.R.; Krauser, J.R.M.; et al. Rhinovirus as the Main Co-Circulating Virus during the COVID-19 Pandemic in Children. *J Pediatr (Rio J)* **2022**, *98*, 579–586, doi:10.1016/j.jped.2022.03.003.
 21. Amarasinghe, G.K.; Aréchiga Ceballos, N.G.; Banyard, A.C.; Basler, C.F.; Bavari, S.; Bennett, A.J.; Blasdell, K.R.; Briese, T.; Bukreyev, A.; Cai (蔡莹芸), Y.; et al. TAXONOMY OF THE ORDER MONONEGAVIRALES: UPDATE 2018. *Arch Virol* **2018**, *163*, 2283–2294, doi:10.1007/s00705-018-3814-x.
 22. Ballegeer, M.; Saelens, X. Cell-Mediated Responses to Human Metapneumovirus Infection. *Viruses* **2020**, *12*, 542, doi:10.3390/v12050542.
 23. Uddin, S.; Thomas, M. Human Metapneumovirus. In *StatPearls*; StatPearls Publishing: Treasure Island (FL), 2022.
 24. Rodríguez, P.E.; Frutos, M.C.; Adamo, M.P.; Cuffini, C.; Cámara, J.A.; Paglini, M.G.; Moreno, L.; Cámara, A. Human Metapneumovirus: Epidemiology and Genotype Diversity in Children and Adult Patients with Respiratory Infection in Córdoba, Argentina. *PLoS One* **2020**, *15*, e0244093, doi:10.1371/journal.pone.0244093.
 25. Stein, M.; Cohen, H.; Nemet, I.; Atari, N.; Kliker, L.; Fratty, I.S.; Bucris, E.; Geva, M.; Mendelson, E.; Zuckerman, N.; et al. Human Metapneumovirus Prevalence during 2019–2021 in Israel Is Influenced by the COVID-19 Pandemic. *International Journal of Infectious Diseases* **2022**, *120*, 205–209, doi:10.1016/j.ijid.2022.04.037.
 26. Elboukari, H.; Ashraf, M. Parainfluenza Virus. In *StatPearls*; StatPearls Publishing: Treasure Island (FL), 2022.
 27. Phan, M.V.T.; Arron, G.; GeurtsvanKessel, C.H.; Huisman, R.C.; Molenkamp, R.; Koopmans, M.P.G.; Cotten, M. Complete Genome Characterization of Eight Human Parainfluenza Viruses from the Netherlands. *Microbiol Resour Announc* **2019**, *8*, e00125-19, doi:10.1128/MRA.00125-19.

28. Zhang, C.; Zhang, K.; Zang, G.; Chen, T.; Lu, N.; Wang, S.; Zhang, G. Curcumin Inhibits Replication of Human Parainfluenza Virus Type 3 by Affecting Viral Inclusion Body Formation. *Biomed Res Int* **2021**, *2021*, 1807293, doi:10.1155/2021/1807293.
29. Trifonova, I.; Christova, I.; Madzharova, I.; Angelova, S.; Voleva, S.; Yordanova, R.; Tcherveniakova, T.; Krumova, S.; Korsun, N. Clinical Significance and Role of Coinfections with Respiratory Pathogens among Individuals with Confirmed Severe Acute Respiratory Syndrome Coronavirus-2 Infection. *Frontiers in Public Health* **2022**, *10*.
30. Kim, D.; Quinn, J.; Pinsky, B.; Shah, N.H.; Brown, I. Rates of Co-Infection Between SARS-CoV-2 and Other Respiratory Pathogens. *JAMA* **2020**, *323*, 2085–2086, doi:10.1001/jama.2020.6266.
31. Kikkert, M. Innate Immune Evasion by Human Respiratory RNA Viruses. *J Innate Immun* **2020**, *12*, 4–20, doi:10.1159/000503030.
32. Clementi, N.; Ghosh, S.; De Santis, M.; Castelli, M.; Criscuolo, E.; Zanoni, I.; Clementi, M.; Mancini, N. Viral Respiratory Pathogens and Lung Injury. *Clin Microbiol Rev* **2021**, *34*, e00103-20, doi:10.1128/CMR.00103-20.
33. Cevik, M.; Tate, M.; Lloyd, O.; Maraolo, A.E.; Schafers, J.; Ho, A. SARS-CoV-2, SARS-CoV, and MERS-CoV Viral Load Dynamics, Duration of Viral Shedding, and Infectiousness: A Systematic Review and Meta-Analysis. *Lancet Microbe* **2021**, *2*, e13–e22, doi:10.1016/S2666-5247(20)30172-5.
34. Fajnzylber, J.; Regan, J.; Coxen, K.; Corry, H.; Wong, C.; Rosenthal, A.; Worrall, D.; Giguel, F.; Piechocka-Trocha, A.; Atyeo, C.; et al. SARS-CoV-2 Viral Load Is Associated with Increased Disease Severity and Mortality. *Nat Commun* **2020**, *11*, 5493, doi:10.1038/s41467-020-19057-5.
35. Ynga-Durand, M.; Maaß, H.; Milošević, M.; Krstanović, F.; Pribanić Matešić, M.; Jonjić, S.; Protić, A.; Brizić, I.; Šustić, A.; Čičin-Šain, L. SARS-CoV-2 Viral Load in the Pulmonary Compartment of Critically Ill COVID-19 Patients Correlates with Viral Serum Load and Fatal Outcomes. *Viruses* **2022**, *14*, 1292, doi:10.3390/v14061292.
36. Hijano, D.R.; Brazelton de Cardenas, J.; Maron, G.; Garner, C.D.; Ferrolino, J.A.; Dallas, R.H.; Gu, Z.; Hayden, R.T. Clinical Correlation of Influenza and Respiratory Syncytial Virus Load Measured by Digital PCR. *PLoS One* **2019**, *14*, e0220908, doi:10.1371/journal.pone.0220908.
37. Walsh, E.E.; Wang, L.; Falsey, A.R.; Qiu, X.; Corbett, A.; Holden-Wiltse, J.; Mariani, T.J.; Topham, D.J.; Caserta, M.T. Virus-Specific Antibody, Viral Load, and Disease Severity in Respiratory Syncytial Virus Infection. *J Infect Dis* **2018**, *218*, 208–217, doi:10.1093/infdis/jiy106.
38. Definiciones_operacionales_de_casos_COVID-19.Pdf.
39. LVL_VR-E_RT-PCR_en_tiempo_real_para_el_diagn_stico_de_SARS-CoV-2_Protocolo_de_Berlin.Pdf.
40. Kodani, M.; Yang, G.; Conklin, L.M.; Travis, T.C.; Whitney, C.G.; Anderson, L.J.; Schrag, S.J.; Taylor, T.H.; Beall, B.W.; Breiman, R.F.; et al. Application of TaqMan Low-Density Arrays for Simultaneous Detection of Multiple Respiratory Pathogens. *J Clin Microbiol* **2011**, *49*, 2175–2182, doi:10.1128/JCM.02270-10.
41. Meskill, S.D.; O'Bryant, S.C. Respiratory Virus Co-Infection in Acute Respiratory Infections in Children. *Curr Infect Dis Rep* **2020**, *22*, 3, doi:10.1007/s11908-020-0711-8.
42. Neumann, G.; Kawaoka, Y. Seasonality of Influenza and Other Respiratory Viruses. *EMBO Mol Med* **2022**, *14*, e15352, doi:10.15252/emmm.202115352.
43. Obando-Pacheco, P.; Justicia-Grande, A.J.; Rivero-Calle, I.; Rodríguez-Tenreiro, C.; Sly, P.; Ramilo, O.; Mejías, A.; Baraldi, E.; Papadopoulos, N.G.; Nair, H.; et al. Respiratory Syncytial Virus Seasonality: A Global Overview. *J Infect Dis* **2018**, *217*, 1356–1364, doi:10.1093/infdis/jiy056.
44. Tempia, S.; Walaza, S.; Bhiman, J.N.; McMorrow, M.L.; Moyes, J.; Mkhencele, T.; Meiring, S.; Quan, V.; Bishop, K.; McAnerney, J.M.; et al. Decline of Influenza and Respiratory Syncytial Virus Detection in Facility-Based Surveillance during the COVID-19 Pandemic, South Africa, January to October 2020. *Euro Surveill* **2021**, *26*, 2001600, doi:10.2807/1560-7917.ES.2021.26.29.2001600.
45. Casalegno, J.-S.; Ploin, D.; Cantais, A.; Masson, E.; Bard, E.; Valette, M.; Fanget, R.; Targe, S.C.; Myar-Dury, A.-F.; Doret-Dion, M.; et al. Characteristics of the Delayed Respiratory Syncytial Virus Epidemic, 2020/2021, Rhône Loire, France. *Euro Surveill* **2021**, *26*, 2100630, doi:10.2807/1560-7917.ES.2021.26.29.2100630.
46. Yeoh, D.K.; Foley, D.A.; Minney-Smith, C.A.; Martin, A.C.; Mace, A.O.; Sikazwe, C.T.; Le, H.; Levy, A.; Blyth, C.C.; Moore, H.C. Impact of Coronavirus Disease 2019 Public Health Measures on Detections of Influenza and Respiratory Syncytial Virus in Children During the 2020 Australian Winter. *Clin Infect Dis* **2021**, *72*, 2199–2202, doi:10.1093/cid/ciaa1475.
47. Li, Y.; Reeves, R.M.; Wang, X.; Bassat, Q.; Brooks, W.A.; Cohen, C.; Moore, D.P.; Nunes, M.; Rath, B.; Campbell, H.; et al. Global Patterns in Monthly Activity of Influenza Virus, Respiratory Syncytial Virus,

- Parainfluenza Virus, and Metapneumovirus: A Systematic Analysis. *The Lancet Global Health* **2019**, *7*, e1031–e1045, doi:10.1016/S2214-109X(19)30264-5.
48. Arellanos-Soto, D.; Padilla-Rivas, G.; Ramos-Jimenez, J.; Galan-Huerta, K.; Lozano-Sepulveda, S.; Martinez-Acuña, N.; Treviño-Garza, C.; Montes-de-Oca-Luna, R.; de-la-O-Cavazos, M.; Rivas-Estilla, A.M. Decline in Influenza Cases in Mexico after the Implementation of Public Health Measures for COVID-19. *Sci Rep* **2021**, *11*, 10730, doi:10.1038/s41598-021-90329-w.
 49. Comte, A.; Bour, J.-B.; Darniot, M.; Pitoiset, C.; Aho-Glélé, L.S.; Manoha, C. Epidemiological Characteristics and Clinical Outcomes of Human Rhinovirus Infections in a Hospitalized Population. Severity Is Independently Linked to RSV Coinfection and Comorbidities. *J Clin Virol* **2020**, *125*, 104290, doi:10.1016/j.jcv.2020.104290.
 50. Chatzis, O.; Darbre, S.; Pasquier, J.; Meylan, P.; Manuel, O.; Aubert, J.D.; Beck-Popovic, M.; Masouridi-Levrat, S.; Ansari, M.; Kaiser, L.; et al. Burden of Severe RSV Disease among Immunocompromised Children and Adults: A 10 Year Retrospective Study. *BMC Infect Dis* **2018**, *18*, 111, doi:10.1186/s12879-018-3002-3.
 51. Pacheco, G.A.; Gálvez, N.M.S.; Soto, J.A.; Andrade, C.A.; Kalergis, A.M. Bacterial and Viral Coinfections with the Human Respiratory Syncytial Virus. *Microorganisms* **2021**, *9*, 1293, doi:10.3390/microorganisms9061293.
 52. Vos, L.M.; Bruyndonckx, R.; Zuithoff, N.P.A.; Little, P.; Oosterheert, J.J.; Broekhuizen, B.D.L.; Lammens, C.; Loens, K.; Viveen, M.; Butler, C.C.; et al. Lower Respiratory Tract Infection in the Community: Associations between Viral Aetiology and Illness Course. *Clin Microbiol Infect* **2021**, *27*, 96–104, doi:10.1016/j.cmi.2020.03.023.
 53. Peng, D.; Zhao, X.; Liu, E.; Huang, Y.; Yang, X.; Zhao, Y.; Chen, X.; Zhang, Z. Analysis of Viral Load in Children Infected with Human Metapneumovirus. *Iran J Pediatr* **2010**, *20*, 393–400.
 54. Kumar, N.; Sharma, S.; Barua, S.; Tripathi, B.N.; Rouse, B.T. Virological and Immunological Outcomes of Coinfections. *Clin Microbiol Rev* **2018**, *31*, e00111-17, doi:10.1128/CMR.00111-17.
 55. Pinky, L.; Dobrovolsky, H.M. Coinfections of the Respiratory Tract: Viral Competition for Resources. *PLoS One* **2016**, *11*, e0155589, doi:10.1371/journal.pone.0155589.
 56. Pinky, L.; Dobrovolsky, H.M. SARS-CoV-2 Coinfections: Could Influenza and the Common Cold Be Beneficial? *J Med Virol* **2020**, *92*, 2623–2630, doi:10.1002/jmv.26098.
 57. JOSHI, P.; SHAW, A.; KAKAKIOS, A.; ISAACS, D. Interferon-Gamma Levels in Nasopharyngeal Secretions of Infants with Respiratory Syncytial Virus and Other Respiratory Viral Infections. *Clin Exp Immunol* **2003**, *131*, 143–147, doi:10.1046/j.1365-2249.2003.02039.x.
 58. Sarkar, S.; Ratho, R.K.; Singh, M.; Singh, M.P.; Singh, A.; Sharma, M. Comparative Analysis of Epidemiology, Clinical Features, and Cytokine Response of Respiratory Syncytial and Human Metapneumovirus Infected Children with Acute Lower Respiratory Infections. *Jpn J Infect Dis* **2022**, *75*, 56–62, doi:10.7883/yoken.JJID.2021.151.
 59. Raita, Y.; Pérez-Losada, M.; Freishtat, R.J.; Harmon, B.; Mansbach, J.M.; Piedra, P.A.; Zhu, Z.; Camargo, C.A.; Hasegawa, K. Integrated Omics Endotyping of Infants with Respiratory Syncytial Virus Bronchiolitis and Risk of Childhood Asthma. *Nat Commun* **2021**, *12*, 3601, doi:10.1038/s41467-021-23859-6.
 60. Shibabaw, T. Inflammatory Cytokine: IL-17A Signaling Pathway in Patients Present with COVID-19 and Current Treatment Strategy. *J Inflamm Res* **2020**, *13*, 673–680, doi:10.2147/JIR.S278335.
 61. Lieberman, N.A.P.; Peddu, V.; Xie, H.; Shrestha, L.; Huang, M.-L.; Mears, M.C.; Cajimat, M.N.; Bente, D.A.; Shi, P.-Y.; Bovier, F.; et al. In Vivo Antiviral Host Transcriptional Response to SARS-CoV-2 by Viral Load, Sex, and Age. *PLoS Biology* **2020**, *18*, e3000849, doi:10.1371/journal.pbio.3000849.
 62. Churiso, G.; Husen, G.; Bulbula, D.; Abebe, L. Immunity Cell Responses to RSV and the Role of Antiviral Inhibitors: A Systematic Review. *IDR* **2022**, *Volume 15*, 7413–7430, doi:10.2147/IDR.S387479.

Disclaimer/Publisher's Note: The statements, opinions and data contained in all publications are solely those of the individual author(s) and contributor(s) and not of MDPI and/or the editor(s). MDPI and/or the editor(s) disclaim responsibility for any injury to people or property resulting from any ideas, methods, instructions or products referred to in the content.